Journal of Optoelectronics and Advanced Materials Vol. 3, Nr. 3, September 2001, p. 703 – 720

AWARD BORIS T. KOLOMIETS

DISCOVERY OF THE INTERMEDIATE PHASE IN CHALCOGENIDE GLASSES

P. Boolchand, D. G. Georgiev, B. Goodman[a]

Department of Electrical and Computer Engineering and Computer Science, University of Cincinnati, Cincinnati, Ohio 45221-0030
[a]Department of Physics, University of Cincinnati, Cincinnati, Ohio 45221-0011

We review Raman scattering, Mössbauer spectroscopy and T-modulated Differential Scanning Calorimetry experiments on several families of chalcogenide glasses. Mean-field constraint theory, and numerical simulations of the vibrational density of state (floppy modes) in random and self-organized networks are used to analyze the measurements. Our results provide evidence for *three* distinct phases of network glasses: *floppy*, *intermediate* and *rigid*, as a function of progressive cross-linking or mean coordination number ($\bar{r}$). These phases are characterized by distinct elastic power-laws. The *intermediate* phase is characterized by a vanishing non-reversing heat-flow, $\Delta H_{nr}(\bar{r}) \rightarrow 0$, suggesting that glass compositions in this phase are configurationally close to their liquid counterparts, i.e. *self-organized.* The compositional width (and centroid) of the *intermediate phase* is found to be determined by glass structure. In *random* networks, the width of the *intermediate phase* almost *vanishes*, and a *solitary floppy* to *rigid* phase transition is observed, in excellent accord with extended constraint theory. In the chalcogenides, some degree of self-organization invariably occurs and opens an *intermediate phase* between the *floppy* and *rigid* phases, signaling the breakdown of mean-field constraint theory, but in harmony with recent numerical results on self-organized networks.

(Received August 23, 2001; accepted September 11, 2001)

Keywords: Intermediate phase, Non-reversing heat flow, Self-organization

1. Introduction

The microscopic origin of glass formation has been debated for over 50 years. It is generally believed that glass formation is a kinetic phenomenon [1], although the aspects of liquid structure that lead to a glass rather than a crystal upon cooling are not obvious at present. Even basic issues on liquid dynamics, such as the propensity of a non-Arrhenius T-variation of viscosity (η), with only a *select few* liquids displaying an exception to that behavior, remains largely a mystery. The challenges to understand glass structures and liquid structures by diffraction methods [2] alone are enormous and have met with limited success. In spite of these challenges, important new ground has been broken particularly in understanding glass structures by using local probes [3] of structures and thermal analysis methods [4]. The latter developments are now beginning to impact our views on liquid structures and dynamics, as we shall see in the present review.

In this review we highlight the elastic (Raman mode frequencies) and thermal response of chalcogenide glasses examined as a function of cross-linking or mean-coordination number, $\bar{r}$. We describe how these experimental results lead in a natural fashion to the existence of three distinct glass phases: *floppy*, *intermediate* and *rigid* that are characterized by distinct elastic power-laws as a function of $\bar{r}$. An important result to emerge from the thermal measurements (Temperature Modulated DSC) is the existence of *compositional windows* [3] across which the non-reversing heat flow, ΔH_{nr}, nearly vanishes. These *windows* are characteristic of glasses in the intermediate phase and are associated with the absence of network stress [5]. Glass transitions become almost completely *thermally reversing* for glass compositions in the intermediate phase. The *intermediate phase* thus becomes synonymous with existence of "*thermally reversing glass compositional windows*", henceforth denoted simply as *windows*. Experiments also reveal that the thresholds in thermal and

elastic behavior coincide [6] and that both are manifestations of glass structure changes as the global connectivity of a network is progressively increased.

For a glass system in which the evolution of network structure with global connectivity is *random*, the window width is found [7] to nearly *vanish* and, correspondingly, an abrupt floppy to rigid transition manifests. The more usual circumstance encountered in glasses is one in where the evolution of cross-linked atomic-scale structures displays some *"self-organization"*, leading to the opening of the window. We shall illustrate this with specific examples.

The discovery of thermally reversing windows has fundamental implications in understanding soft matter. The absence of network stress in the intermediate phase is associated with *facile photomelting* of that phase under optical illumination. This could relate to the observation of photomelting [8] in As_2S_3 glass and the giant photocollapse [9] of obliquely deposited porous $GeSe_2$ films [9]. Both glass systems are intrinsically phase separated on a molecular scale. In both cases the chalcogen-rich phase is thought to undergo a photomelt.

There are also early indications that glass compositions in the *intermediate phase* heated past T_g, display an Arrhenius T-variation of viscosity. Such a variation is characteristic of *strong* liquids, in the strong-fragile classification [10].

In *section 2*, we comment on overview of the theoretical tools employed to analyze the elastic response of glasses. In *section 3*, we provide experimental results on four families of chalcogenide glasses where intermediate phases are documented, in some cases by both Raman scattering and MDSC measurements. The special case of the chalcohalide Ge-S-I with dangling-bond structure is discussed in *section 4*. In *section 5*, we provide evidence of photomelting in the intermediate phase of the Ge_xSe_{1-x} binary glass system. We conclude in *section 6* with a summary of the principal results.

2. Rigidity transition in random networks – theory

2.1 Basic ideas

An important step to understand glasses at a basic structural level emerged in 1979 when J. C. Phillips introduced ideas based on mechanical-constraint counting [11] algorithms to explain glass forming tendencies in network forming systems. He reasoned that for a liquid to form a glass composed of a network possessing well-defined local structures, interatomic forces must form a hierarchical order. The strongest covalent forces between nearest neighbors serve as Lagrangian (mechanical) constraints defining the elements of local structure (building blocks). Constraints associated with the weaker forces of more distant neighbors must be intrinsically broken leading to the absence of long-range order. He speculated that the glass forming tendency is optimized when the number of Lagrangian local-bonding constraints per atom, n_c, just equals the number of degrees of freedom. For a 3d network,

$$n_c = 3 \tag{1}$$

In covalent solids, there are two types of near-neighbor bonding forces; bond-stretching (α-forces) and bond-bending (β-forces). The number of Lagrangian bond-stretching constraints per atom is $n_\alpha = r/2$, and of bond-bending constraints is $n_\beta = 2r-3$. For the case when all α- and β-constraints are intact and no dangling ends (one-fold coordinated atoms, $n_1/N = 0$) exist in the network, equation (1) implies that the optimum mean coordination number is $\bar{r} = 2.40$. Highly overcoordinated or undercoordinated structures are not conducive to glass formation and, upon cooling, lead to crystalline solids. Phillips' speculation is in excellent accord with the general experience on glass formation in inorganic solids.

In 1983, M. F. Thorpe pointed [12] out that undercoordinated networks would possess, in the absence of the weaker longer range forces, a finite fraction of zero-frequency normal vibrational modes, the *floppy modes*. In fact, he found from simulations on random networks that the number of floppy modes per atom, f, is rather accurately described by the mean-field constraint count according to the relation,

$$f = 3 - n_c \tag{2}$$

This led to the realization that a glass network will become spontaneously rigid when $f \rightarrow 0$, defining a *floppy* to *rigid phase transition*. Fig. 1 shows a plot of f against $\bar{r}$ for the cases of two random networks, one generated by scission of an amorphous Si network and the other by scission of an amorphous (C) diamond network. In both instances, the second derivative of f with $\bar{r}$ shows [13] a fairly sharp *cusp* at $\bar{r}_c$ (C) = 2.375(3) and $\bar{r}_c$ (Si) = 2.385(3), respectively, quite close to the mean-field value of $\bar{r}_c$ = 2.40. The numerical simulations also reveal an exponential tail to f($\bar{r}$) at $\bar{r} > \bar{r}_c$. In contrast the mean-field calculations give a linear variation of f($\bar{r}$) till zero at $\bar{r}_c$ = 2.40, and f = 0 for $\bar{r} > \bar{r}_c$.

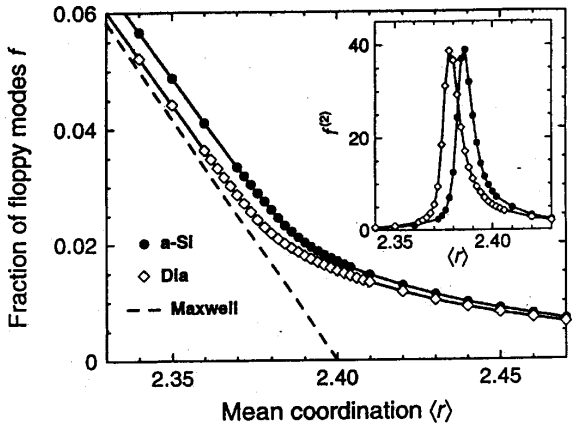

Fig. 1. The number of floppy modes per degree of freedom, f, for two bond-diluted models, based on the diamond lattice and on amorphous Si. The inset shows the second derivative of f with respect to <r> for the same models (Ref. 13). The broken line gives the predicted linear variation for mean-field constraint counting (Maxwell).

A significant result of these numerical simulations on random networks is the prediction of a rather robust *power-law variation* of elastic constants [14, 15] C (longitudinal, transverse and shear) as a function of $\bar{r}$,

$$C = A(\bar{r} - \bar{r}_c)^p \tag{2}$$

in the *rigid regime* with p = 1.4 -1.50. We shall return to this prediction later.

2.2 Broken bond-bending (β) constraints

In glasses one rarely observes [4] the solitary rigidity transition $\bar{r}_c$ = 2.40 as discussed above. In part, this is because glasses soften at a finite temperature T_g, in contrast to the constraint and harmonic elasticity theory predictions which are based on T = 0 K calculations. Since α-forces exceed β-forces by a factor of 3 or more, in glass systems possessing a high T_g and/or weak β-forces, constraints associated with β-forces may be intrinsically *broken* [16, 17]. For a network with a finite fraction (m_r/N) of r-fold (r ≥2) coordinated atoms that have their β-constraints broken, the mean-field rigidity transition will be upshifted [4] in $\bar{r}$ according to

$$\bar{r}_c = 2.40 + \frac{2}{5}\left(\frac{m_2}{N}\right) + \frac{6}{4}\left(\frac{m_3}{N}\right) + 2\left(\frac{m_4}{N}\right) \tag{3}$$

SiO_2 glass is a celebrated example of a network where the β-constraint associated with the bridging O atoms is intrinsically broken. This is due to the rather high T_g = 1200°C, of SiO_2 which leads thermal energies at T_g to completely overwhelm the strain energy barrier associated with a sharply defined O-bridging angle. The result is a wide distribution of the bridging O-bonding angle as inferred from diffraction experiments [18]. In this case, $m_2/N = 2/3$, the fraction of oxygen atoms per formula unit and according to Eq. (3), the condition $n_c = 3$ now occurs at $\bar{r} = 2.67$ since $m_3/N = m_4/N = 0$. The propensity toward glass formation in this prototypical oxide derives from the fact that the stoichiometric SiO_2 glass composition is optimally constrained [17] even though $\bar{r} = 2.67$!

A second example is the case of the $Ge_{1-x}Sn_xSe_2$ ternary in which the β-forces associated with the lighter Ge group IV atom are much *stronger* than those associated with the heavier and more metallic group IV atom Sn. The result is that the β-constraints associated with all Sn-atoms at Tg $\simeq$ 200°C are broken, and a rigidity transition is predicted by (3) to be at

$$1/3[4(1-x) + 4(x) + 4] = 2.40 + 2x/3$$

$$\text{or } x_c = 2/5 \tag{4}$$

Here $m_2/N = m_3/N = 0$ and $m_4/N = x$. The predicted threshold [19] is quite close to the observed threshold ($x_c = 0.35$) in ^{119}Sn Mössbauer spectroscopy measurements [20] on these ternary glasses.

2.3 Networks with dangling ends

Halogens in covalently bonded systems and hydrogen in Si are some familiar examples of networks with dangling ends, i.e., atoms that are one-fold coordinated (OFC). The mean-field constraint counting is modified as follows: for an atom with r > 1

$$n_\alpha = r/2 \tag{5a}$$
$$n_\beta = 2r - 3 \tag{5b}$$

For an OFC atom there is no β constraint and the rigidity transition condition ($n_c = 3$) now occurs when

$$\bar{r}_c = 2.40 - 0.4(n_1/N) \tag{6}$$

leading in general to a downshift [21] of the threshold from the magic value of 2.40. In general, OFC-atoms play no role if the base glass network (without one-fold coordinated atoms) is optimally coordinated [22]. On the other hand, these atoms will soften [23] an overconstrained base network and conversely stiffen [22] an underconstrained base glass network.

2.4 Rigidity transitions in self-organized networks

In our discussion so far, we have not distinguished between onset of *rigidity* from onset of *stress*. A network can be *isostatically rigid*, that is, with no stress present. Stresses are said to exist when already present bond lengths and/or angles must change on the addition of more atoms to the structure. Thus, the imposition of additional cross links or constraints can lead to *redundant constraints* and to the accumulation of *stress*. An example can serve to illustrate the idea. Consider 4 elastic bars hinged at their ends to form a square. A square is not a rigid structure because it can be sheared into a rhombus. A crossbar attached to opposite vertices of the square will result in an isostatically (barely) rigid structure. A second crossbar attached across the remaining two vertices provides a redundant constraint and will result in accumulation of stress in the structure. Isostatically rigid and stressed rigid random structures are expected to be physically different in behavior, as we now discuss.

Let us consider a cross-linked random network with $\bar{r}$ = 2.2 so that it consists of floppy regions and sparsely populated isostatically rigid inclusions. Next we insert additional cross-links in a *selective* fashion; we allow a cross-link in the floppy segment of the network, but not in an isostatically rigid region to avoid redundant constraints and stress. The process is a form of self-organized growth. The question remains, how far can we proceed before stressed rigidity manifests itself. The issue was recently addressed in a numerical simulation of self-organized growth by M.F. Thorpe et al. who found [23] that, in a scissoned amorphous Si Network, isostatic rigidity manifests at $\bar{r} = \bar{r}_c(1) = 2.375(15)$ while stressed rigidity onsets at $\bar{r} = \bar{r}_c(2) = 2.392(15)$ as shown in Fig. 2. In a real system, self-organization process may be driven by free energy of a glassy melt. These simulations [23] suggest that there are *two transitions*, a floppy to an isostatically rigid state followed by an isostatically rigid to a stressed rigid state. Glass compositions residing between the floppy and stressed rigid phase define the *intermediate phase*. These simulations are in sharp contrast to those on random networks that predict [13] the stress and rigidity transition to coincide and occur at a unique value of $\bar{r}$.

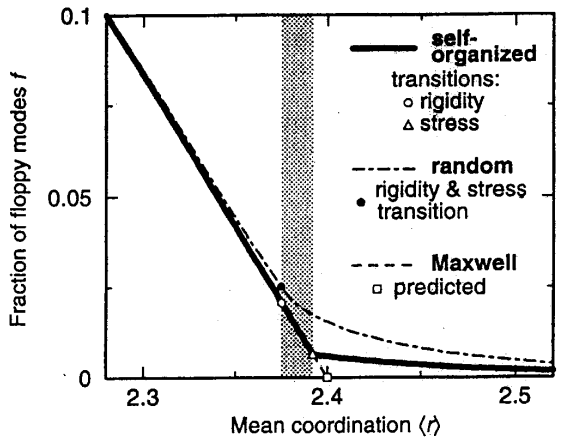

Fig. 2. The fractions of floppy modes per degree of freedom for the diluted diamond lattice for the random case (broken line) and the self-organized case (solid line). For the self-organized case the rigidity transition (o) and the stress transition (D) rise to the intermediate phase shown as the shaded region. Fig. taken from Ref. 13.

Raman and MDSC experiments on chalcogenide glasses provide evidence of two rigidity transitions, as we shall describe next in *section 3*. There is at present a significant difference with respect to the values of $r_c(1)$ and $r_c(2)$ between the numerical model and experiments. Still these new numerical simulations represent a significant advance and provide a physical basis for characterizing the nature of the two transitions and some insights into the *self-organized* intermediate state.

3. Experimental probes of rigidity transitions

Different types of experimental methods have given evidence on the nature of rigidity transitions in glasses. These include T-modulated Differential Scanning Calorimetry [4], Raman [4, 24] and Brillouin scattering [25], Neutron scattering [29], and Mössbauer spectroscopy [26], viscosity [27], thermal expansion [28], and Molar volume measurements. Anomalies in compositional trends of electronic behavior of glasses near the rigidity transition have also been observed, such as the semiconductor to metal transition pressures [30] and electric fields for electronic switching [31]. The connection between electronic behavior and glass structure remains to be understood in this context, however.

3.1 Thermally reversing windows and the intermediate phase

Differential Scanning Calorimetry (DSC) has been used to establish glass transition temperatures, T_g, for the past 50 years. Although the glass transition itself is quite wide (> 20°C), one can usually localize the inflexion point of the heat flow endotherm to within ±2°C, and thus define T_g. However, it is well known that not only does the shape of the heat flow endotherm depend on the baseline of the instrument, but also on the thermal history of the sample and the scan rate employed. Several of these limitations have been overcome in a recent variant of DSC known as MDSC. In the latter, the programmed heating rate [32] includes a sinusoidal T-modulation superimposed on a linear T ramp used to scan through the glass transition. Because of increased sensitivity, an order of magnitude reduction in scan rates (1-3°C/min) can be used in MDSC in relation to those (10-20°C/min) used in DSC. Furthermore, in MDSC it is possible to deconvolute the total heat-flow rate into a part that tracks the T-modulation and is known as the *reversing heat flow rate*, leaving a part that does not track the T-modulation, which is known as the *non-reversing heat-flow rate*.

Experience on a wide variety of glass systems shows that the non-reversing heat-flow rate displays a Gaussian-like peak as a *precursor* [2] to the glass transition. The latter is observed as a smooth step-like shift of the reversing heat-flow rate as illustrated in Fig. 3.

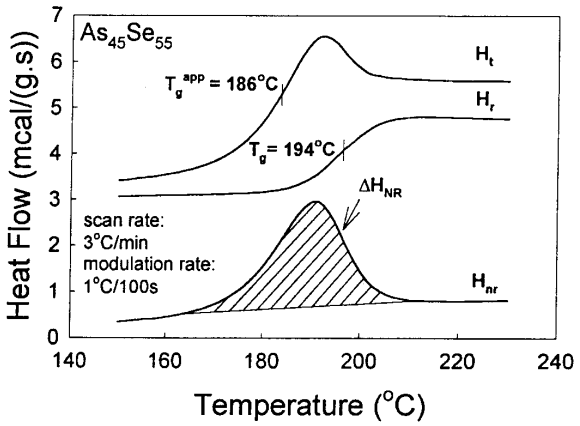

Fig. 3. MDSC scan of $As_{45}Se_{55}$ glass showing deconvolution of the total heat flow H_t into reversing, H_r, and non-reversing, H_{nr}, components. Fig. is taken from Ref. 34.

The area under the non-reversing heat flow rate will be denoted henceforth as ΔH_{nr}, *the non-reversing heat-flow*. ΔH_{nr} is thermal history sensitive. It is found to saturate in time typically after 100 hours to a fully relaxed glass. In this work, ΔH_{nr} is *used to denote* the *saturated* value, and it measures the latent heat between the relaxed solid glass and its melt. The sigmoidal jump in the reversing heat flow observed in these experiments is *independent of the baseline of the instrument*. It establishes the thermodynamic jump ΔC_p in the specific heat between the glass and its melt and its inflection point can be taken to define T_g. Furthermore, by scanning up and then down in T across T_g, one can correct for the small but finite scan-rate-dependent shift of T_g and thus obtain *scan-rate independent* T_g and ΔH_{nr}. Such T_g's, independent of scan rates and sample thermal history, are closely correlated with glass compositions [5, 33, 34]. Compositional trends in T_g provide a measure of global connectivity of the network, an idea that has been made quantitative in the past few years by stochastic agglomeration theory [35]. The ΔH_{nr} term provides a measure of how different a glass is from the liquid in a configurational sense. For glass compositions in the *intermediate phase*, ΔH_{nr} term is found to nearly *vanish*. This unequivocally suggests that glass- and liquid-structures in the window compositions are *closely similar* to each other and that both are *stress free* in a global sense.

In Fig. 4, we provide examples of thermally reversing windows observed in chalcogenide glasses. In the Ge_xSe_{1-x} binary, the ΔH_{nr} term is found [16] to *decrease* by almost an order of

magnitude in the $0.20 < x < 0.26$ (or $2.40 < \bar{r} < 2.52$) composition region (indicated by a pair of arrows). This composition range serves to define the thermally reversing window in this binary. We will revisit these results in conjunction with Raman results later.

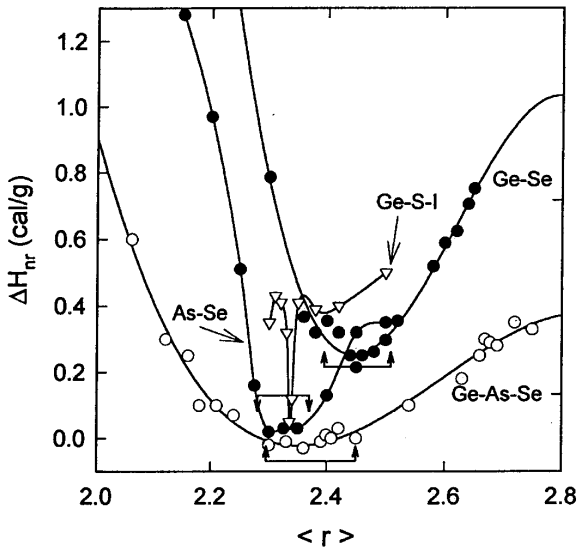

Fig. 4. Non-reversing heat, DH_{nr},as a function of mean coordination number <r> for four different glass systems. The Ge-As-Se ternary shows the widest window (Ref. 5) while the Ge-S-I the narrowest (Ref. 7).

In the As_xSe_{1-x} binary the window centroid is somewhat shifted [34] to lower $\bar{r}$, $2.29 < \bar{r} < 2.37$. This is a surprising result, given the fact that the stoichiometric glass As_2Se_3 corresponds to $\bar{r} = 2.40$ and is widely viewed to be an optimally coordinated, chemically ordered, and continuous random network of $As(Se_{1/2})_3$ pyramids. This, along with the non-Arrhenius T-variation [1] of viscosity of liquid As_2Se_3, suggests that the traditional view cannot be the complete picture and that the stoichiometric glass is neither *completely chemically ordered* nor is it optimally coordinated. The difference appears to be associated with an intrinsic nanoscale phase separation into As-rich and Se-rich clusters, as is suggested by local-probe results and by the T_g maximum near $x = 2/5$. The fact (Fig. 4) that As_xSe_{1-x} glasses in the $0.29 < x < 0.37$ composition range appear to be *optimally coordinated* is incompatible with *presence of* pyramidal $As(Se_{1/2})_3$ units being the only As-centered local units in the Se-rich glasses ($x < 0.40$). The shift of the window to $x < 0.40$ suggests that quasi-tetrahedral units of the type $Se = As(Se_{1/2})_3$ in which the valence of As is formally 5+, are probably also present. The attractive feature of these quasi-tetrahedral units is that the number of constraints per atom for such a unit is *exactly* 3, even though the unit is undercoordinated ($\bar{r} = 2.285$). This special circumstance arises because of the terminal (non-bridging) Se atom. In the P_xSe_{1-x} binary, one also observes a thermally reversing window [33] in the same cation concentration range. In this binary, there is evidence for 4-fold coordinated P from NMR measurements [36].

The thermally reversing window in the $Ge_xAs_xSe_{1-2x}$ ternary is widest [5] of the four chalcogenide glass systems presented in Fig. 4. Here one can expect the ternary to be made up of several types of optimally coordinated building ($n_c = 3$) blocks, $As(Se_{1/2})_3$ pyramids, $Se = (As)(Se_{1/2})_3$ quasi-tetrahedra, Se_n chain segments with corner-sharing $Ge(Se_{1/2})_4$ tetrahedra. The increased number of optimally coordinated units in this ternary opens new possibilities to form the elements of medium-range structure in a self-organized backbone. It is for this reason, we believe, that the window is rather wide in the ternary.

The spectacularly narrow window found [7] in the $Ge_{0.25}S_{0.75-y}I_y$ ternary puts in perspective the large width of windows seen in the binary and ternary chalcogenides. We shall discuss the special case of this chalcohalide in section 5. It appears to be a model example of a *random network* and the

collapse of the thermally reversing window is due to absence of self-organization in this "random" network.

In summary, thermally reversing windows deduced from MDSC measurements serve to define the extent of the *intermediate phase* present in ternary As-Ge-Se glasses as sketched in the phase diagram of Fig. 5. The *intermediate phase* opens up in between the *floppy* and *rigid* phases and near glass compositions corresponding to $\bar{r} = 2.40$. The results of Fig. 5 showcase the central *new result* of this work. These thermal thresholds are found to coincide with elastic thresholds deduced from Raman optical elasticities on these glasses, as we shall discuss next.

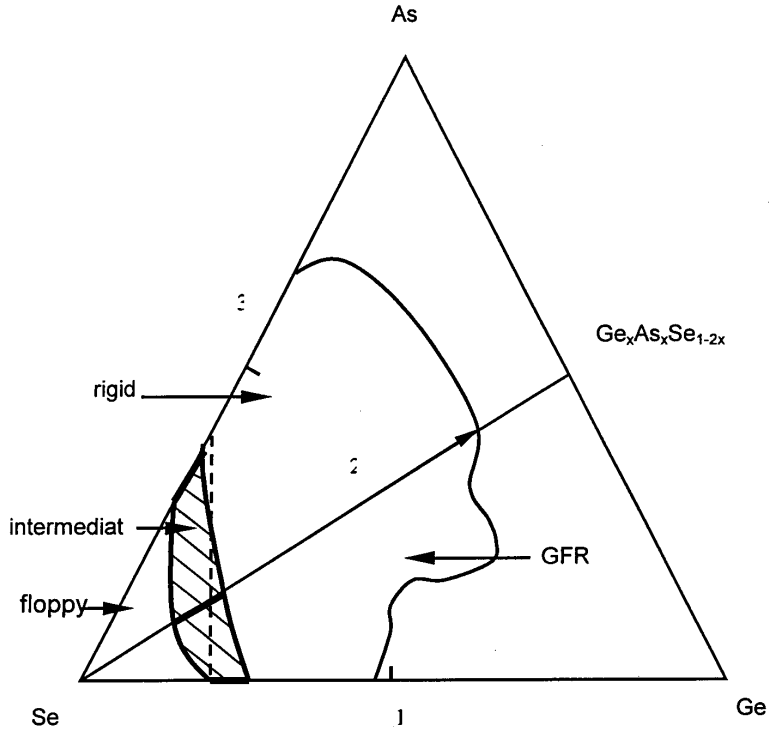

Fig. 5. The glass-forming region in the Ge-As-Se ternary glass system. The broken line corresponds to <r> = 2.40. The shaded region gives the opening of the intermediate phase between the floppy and the rigid phases, and it straddles the <r> = 2.40 line.

3.2 Raman scattering, elastic thresholds and the intermediate phase

Although Raman scattering has been widely used as a probe [37-40] of glass structure for the past three decades, its application as a probe of the *rigidity transitions* in network glasses is a *recent* [4, 6, 16] development. In many cases, when vibrational bands associated with a specific network building block can be resolved in the Raman lineshapes, it is possible to quantitatively follow mode frequency changes with glass composition. And although the scale of mode frequencies are set by the strength of α- and β-forces, shifts in mode frequencies with glass compositions result from inter-building-block couplings. Raman scattering experiments on several IV-VI glass systems have now been performed [6, 16]. These comprehensive results provide supporting evidence for two rigidity ($r_c(1)$, $r_c(2)$) transitions in these chalcogenide glasses, in that elastic thresholds correlate well with thermal thresholds deduced from MDSC measurements.

A plot of the CS mode frequency (ν_{CS}) in Ge_xSe_{1-x} glasses as a function of Ge concentration yields kinks [41] near $x_c(1) = 0.20$ and $x_c(2) = 0.26$ as shown in Fig. 6. For glass compositions at $x > x_c(2) = 0.26$, we have fit to an underlying elastic power-law by plotting ν_{CS}^2 against $\bar{r} - \bar{r}_c(2)$ on a

loglog plot, and obtain a power-law of p = 1.54(10) as shown in Fig. 7. The result is reminiscent of the numerical simulations [23] of elastic constants in random networks constrained by α- and β-forces for which p in the rigid regime is predicted to be 1.40 - 1.50. These results provide unambiguous evidence for the onset of a new rigidity at $x_c > 0.26$.

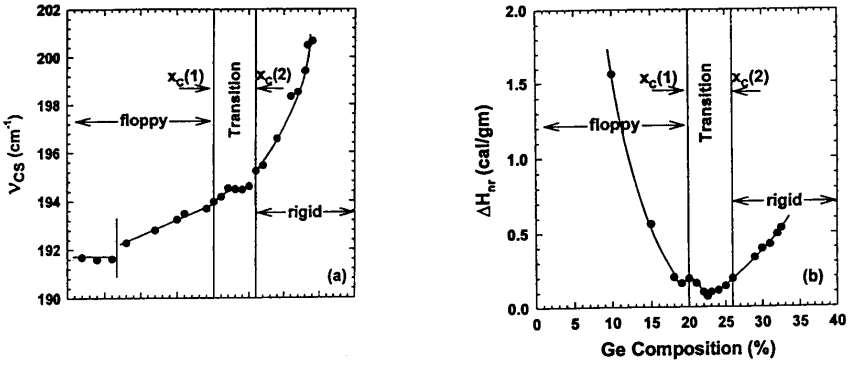

Fig. 6a). Raman mode frequency variation of corner-sharing (n_{CS}) tetrahedra in Ge_xSe_{1-x} plotted as a function of x; b) Non-reversing heat variation, $DH_{nr}(x)$, in Ge_xSe_{1-x} glasses. Fig. is taken from Ref. 41.

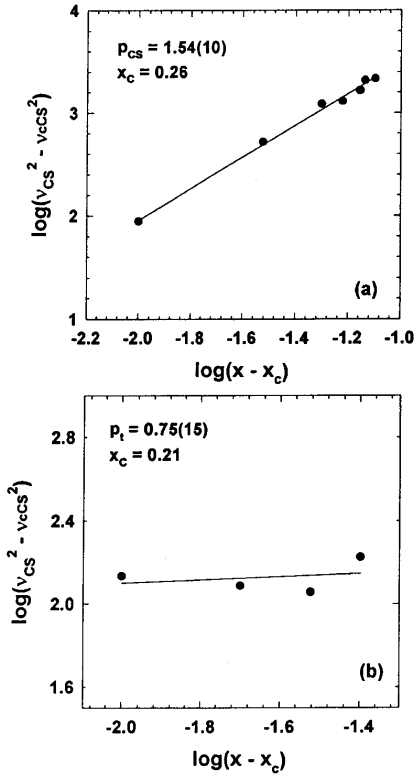

Fig. 7. Plots of $\log_{10}(n^2 - n^2_C(x))$ against $\log_{10}(x - x_C)$ for the CS mode frequency in Ge_xSe_{1-x} glasses. The plots give respective power laws for CS - mode - based optical elasticity in the rigid region, p_{CS}, and in the transition region, p_t. Fig. taken from Ref. 41.

In the $0.20 < x < 0.26$ composition range, a similar fit of the CS mode frequency squared against $\bar{r} - \bar{r}_c(1)$ on a loglog plot, yields a much lower value of $p = 0.75(15)$. Such a sub-linear power-law may be compared to the finite scaling result [42] which is $2/d = 2/3$ for $d = 3$ (3d network). To obtain a power-law $p < 1$, one must invoke large-scale or long-range fluctuations as are discussed in equilibrium-scaling theory.

A distinctly different elastic behavior is suggested in the $0.10 < x < 0.20$ composition range from the Raman measurements, namely a linear $\nu_{CS}(x)$ variation. Furthermore, at $x < 0.07$, Raman measurements show $\nu_{CS}(x)$ to become independent of x, a regime in which the $T_g(x)$ variation is found to be linear [41, 43] with a slope ($dT_g/dx = T_o/\ln 2$). In the lowest x (< 0.07) regime, the $T_g(x)$ trends, $\nu_{CS}(x)$ trends, and Mössbauer site-intensity ratios in ^{129}I spectroscopy [44], all point to a *stochastic regime* of agglomeration in which CS $Ge(Se_{1/2})_4$ units *randomly* cross-link Se_n-chain segments to define a floppy phase of these binary glasses. In the $0.10 < x < 0.20$, ES tetrahedral units may appear in addition to CS ones and precipitate nuclei of isostatically rigid inclusions in which more extended-range structural correlations evolve. In this particular regime the challenges are more formidable and our current understanding of $T_g(x)$ trends, $\nu(x)$ trends continues to be qualitative. More work is needed to understand the underlying behavior.

The compositional trends in $\nu_{CS}(x)$ and $\Delta H_{nr}(x)$ as seen in Raman and MDSC measurements are shown in Fig. 6. There are clear correlations between these trends, which are driven by aspects of glass structure. In particular, the $\nu_{CS}(x)$ variation of Fig. 6 shows that the rigidity transition near $x_c(1) = 0.20$ appears to be continuous, i.e., second order, while the stress transition near $x_c(2) = 0.26$ discontinuous or first order. Thorpe et al. [45] have suggested that the network rigidity nucleates at small rings, $n < 6$. Numerical simulations in networks that possess no rings, such as *random bond networks* [45] and *Bethe lattices*, [46] show a *first order* transition to a stressed backbone structure. Stressed rigidity is believed to nucleate in n-membered rings with $n < 6$ in general. These results suggest that in the binary Ge_xSe_{1-x} glasses the concentration of small rings, $n = 5, 4$, must be quite small at $x < 0.26$ for the transition to be first order.

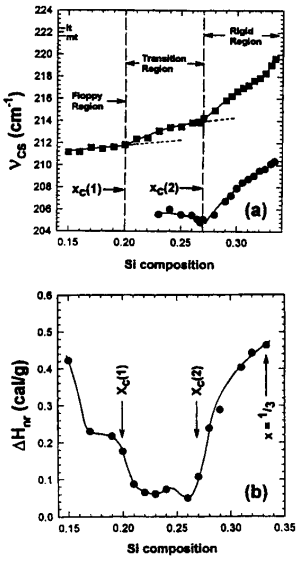

Fig. 8a). Raman mode frequency variation of corner-sharing (n_{CS}) tetrahedra in Si_xSe_{1-x} plotted as a function of x; b) Non-reversing heat variation, $DH_{nr}(x)$, in Si_xSe_{1-x} glasses. Both observables show the opening of the intermediate phase in the $x_c(1) < x < x_c(2)$ region. Fig. is taken from Ref. 6.

Fig. 8 shows parallel Raman and MDSC results to Fig. 6 for the Si_xSe_{1-x} binary glass system taken from ref. 6. The correlation between the elastic and the thermal-thresholds is rather *compelling* in this system, probably because the glass structure is dominated by chains of ES tetrahedra. The *intermediate phase* extends from $x_c(1) = 0.20$ to $x_c(2) = 0.26$, quite similar to the one seen [41] in the Ge_xSe_{1-x} binary.

3.3 Lamb-Mössbauer factors and rigidity transition in glasses

Mössbauer spectroscopy has served as a powerful, local probe [47] of glass structure. The Mössbauer hyperfine structure observed in glasses provides means to probe the local environment of the resonant nucleus/atom. Furthermore, the T-dependence of the integrated area under a nuclear resonance through measurements of the Lamb-Mössbauer factor, has proved to be a useful probe [26] of *low-frequency vibrational excitations* in glasses. Thus, both the static and dynamic structures about a resonant atom in a network glass can be elegantly probed. This subject has been reviewed elsewhere, the interested reader is referred to those publications [47].

3.4 T-dependence of viscosity and the intermediate phase

The T-dependence of viscosity of glass forming liquids has been studied [48] for the past 30 years. Liquids are classified as *strong* [49] if an Arrhenius T-dependence of viscosity is observed, and are *fragile* if a strongly non-Arrhenius T-dependence of viscosity is observed. An elegant means of presenting these results is on a plot of log η against 1/T normalized to T_g, as illustrated in Fig. 9a for melts of the As-Se binary glass system. These results are taken from the work of Nemilov and Petrovckii [50]. In Fig. 9b, the dark circles are the activation energy for viscosity, $E_\eta^A(x)$ at T_g. In this figure we have also superposed (open circles) the compositional trend in $\Delta H_{nr}(x)$ taken from our work.

Fig. 9 demonstrates that compositional trends in $E_\eta^A(x)$ track those in $\Delta H_{nr}(x)$, a pattern observed in two other glass systems where the results are available. Glass compositions in the intermediate phase, upon melting, display an Arrhenius T-variation of viscosity, i.e., give rise to *strong liquids*. On the other hand, both floppy and rigid glasses give rise to *fragile liquids* with a strongly non-Arrhenius T-variation of viscosity.

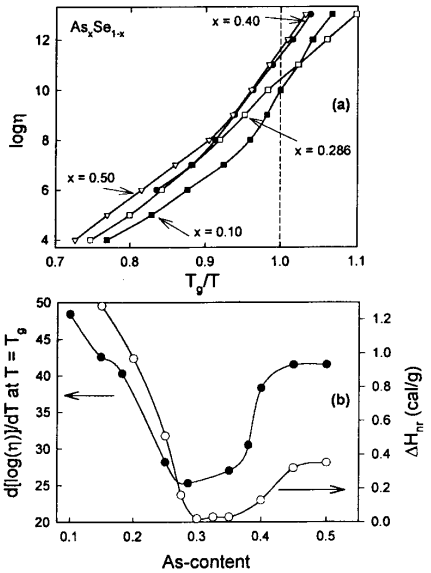

Fig. 9a). Plot of log η against 1/T normalized at T_g taken from ref. 50. (b) Non -reversing heat, DH_{nr}, and the activation energy for viscosity d(log(h))/dT at T_g ,in As_xSe_{1-x} glasses as a function of As content. Note both observable track each other suggesting that the glass softening behavior carries the memory of liquid dynamics.

The central message underlying the correlation of Fig. 9 may be summarized. The viscosity η of a liquid provides a measure of the shear relaxation time (τ_s) through the Maxwell relation,

$$\eta = \tau_s G_\infty \tag{7}$$

where G_∞ is the high-frequency shear modulus. Since G_∞ is known to be largely T-independent, E_η^A thus also serves as an activation energy for shear relaxation time in a liquid. The correlation observed in Fig. 9 shows a connection between the glass structure and *liquid dynamics*. It is becoming increasingly clear that concepts of global connectivity developed to describe glass networks extend well into the liquid state, conversely, that the underlying dynamics of structural arrest of a liquid on solidification is related to the global connectivity of the liquid structure. The discovery of the intermediate phase thus allows us for the first time to correlate the *strong-fragile* classification [49] of liquids with the *floppy-intermediate-rigid* classification of glasses. Glasses in the *intermediate phase* give rise to *strong* liquids. Glasses in both the *floppy* and *rigid* phases give rise to *fragile* liquids. *Fragility* is thus a multivalued concept and needs to be refined. Since both floppy and rigid glasses give rise to fragile liquids, it remains to be understood in what manner does the T-dependence of viscosity of floppy liquids differ from that of rigid liquids.

We conclude this section with two remarks. First, As_2Se_3 glass is often regarded as an optimally coordinated ($\bar{r}$ = 2.40, $\overline{n_c}$ = 3) glass network. Surprisingly, neither the T-dependence of melt viscosity nor the measured ΔH_{nr} puts this composition in the thermally reversing window, although it is not far away (Fig. 9b). The small deviation of this glass composition away from the edge of the thermally reversing window suggests that the glass is slightly overconstrained relative to its putative composition. Such a result can arise if the glass network is intrinsically *phase separated* into Se-rich and As-rich regions with the latter phase comprising the rigid backbone.

Second, systematic studies of the T-dependence of viscosities of chalcogenide liquids as a function of composition are likely to provide important insights into aspects of nanoscale phase separation in the liquid state that apparently not only control the dynamics in the liquid state but also the nature of the structurally arrested state in the glass.

4. A very narrow thermally reversing window in $Ge_{0.25}S_{0.75-y}I_y$ glasses

Additional insights into the molecular origin of thermally reversing windows in network glasses have recently emerged from studies on the chalcohalides [51] Ge-S(or Se)-I. Here we start with a marginally rigid base glass of $Ge_{0.25}S_{0.75}$ composition and systematically replace S by I, to get ternary $Ge_{0.25}S_{0.75-y}I_y$ glasses in the $0 < y < 0.30$ concentration range. The global glass forming tendency in this ternary was recognized by Dembovsky [52], and the present compositions reside in that part of the phase diagram where the glass forming tendency is actually rather high [21]. One expects I to chemically bond with Ge because of Pauling charge transfer effects and to replace bridging S with terminal I in the backbone. The replacement converts tetrahedrally coordinated CS $Ge(S_{1/2})_4$ units (m = 0 units) into mixed tetrahedral units of the type $Ge(S_{1/2})_{4-m}I_m$ with m = 1, 2, 3 and eventually 4, as y is systematically increased. The m = 4 units form monomers, GeI_4 molecules, that are decoupled from the backbone.

MDSC experiments on this system show $T_g(y)$ to systematically decrease with y at first slowly in the $0 < y < 0.15$ range and then sharply in the $0.15 < y < 0.17$ range as shown in Fig. 10. In the $0 < y < 0.15$ concentration range stochastic agglomeration theory permits a quantitative analysis of the $T_g(y)$ trends through the ways in which the various m-units combine or agglomerate to form the backbone. But the central result to emerge from these MDSC measurements is the compositional dependence of $\Delta H_{nr}(y)$ which has a *sharply* defined *global minimum* centered at $y = y_c = 0.162(4)$ (corresponding to $\bar{r}$ = 2.34 of the ternary). In the estimate of $\bar{r}$, we take the r of Ge, S, and I to be 4, 2 and 1, respectively.

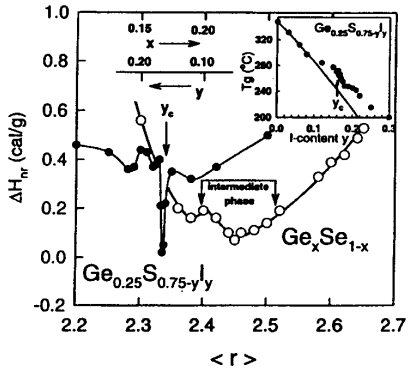

Fig. 10. Variation of the non-reversing heat flow, DH_{nr}, as a function of <r> in the ternary $Ge_{0.25}S_{0.75-y}I_y$ and in the binary Ge_xSe_{1-x}. The inset shows the $T_g(y)$ variation in the ternary and the smooth line is the prediction of the agglomeration theory. Fig is taken from Ref. 7.

According to equation 6, mean-field constraint counting for the $Ge_{0.25}S_{0.75-y}I_y$ ternary is

$$\bar{r}_c = 2.40 - 0.4y_c \tag{8a}$$

or

$$4(1/4) + 2(3/4\text{-}y_c) + 1(y_c) = 2.40 - 0.4y_c$$

$$y_c = 1/6 = 16.6 \tag{8b}$$

in excellent accord with the value of $y_c = 0.162(4)$ observed for the minimum in $\Delta H_{nr}(y)$.

The physical picture emerging from these MDSC measurements is that iodine alloying in the marginally rigid base glass, $Ge_{0.25}S_{0.75}$ steadily de-polymerizes the backbone thereby leading to a reduction in T_g. Near $y_c = 0.162$, there is a precipiteous reduction in T_g, and ΔH_{nr} shows a global minimum corresponding to a sharply defined rigid to floppy transition that is in excellent accord with extended mean-field constraint theory.

Obvious questions arise: why is the rigid to floppy transition so *sharp* in this chalcohalide glass system? Why is the threshold in perfect agreement with constraint theory? Raman scattering results on these glasses provide important clues [7] to address these issues. Through them one can quantitatively decode the concentrations $N_m(y)/N$ of the various m-units from the relative strengths of the Raman peaks identified [53] with the symmetric stretching modes of the m = 0, 1, 2, 3 and 4 quasi-tetrahedra. Fig. 11 provides a plot of trends in $N_m/N(y)$ deduced from the Raman results. On this plot we have also included the predicted variation of the N_m/N concentrations (smooth lines) if the iodine alloying were to proceed *randomly* according to combinatorial calculations. Here one cannot overemphasize that the smooth lines are *not a fit to the data* but merely the prediction of the combinational calculations. The excellent agreement between theory and experiment up to y = 0.17 carries a central message: evolution of the Ge-S backbone upon progressive alloying with I for S proceeds in a truly *random* fashion up to the phase transition. In glass science it is popular to invoke continuous random networks. Our experiments here show that it is actually rare ($Ge_{0.25}S_{0.75-y}I_y$ being one of the exceptions) that glass networks are random and continuous.

Returning back to the rigidity transition, one can now unambiguously relate the *sharpness* of the phase transition to the *stochastic evolution* of the backbone that precludes self-organization and formation of extended range structures composed of rings. In turn these results suggest that the large width of the intermediate phase encountered in the Ge_xSe_{1-x} binary (see Fig. 11) and other glasses (Fig. 4), is probably the result of substantial structural reorganization of the backbone when the latter is optimally constrained. Some of the structural reorganization taking place may consist of optimally constrained filamentary structures that pack well and globally lower molar volumes of these glass compositions [29]. The decoupling of these filamentary structures may intrinsically contribute to a lowering of the ΔH_{nr} term by avoiding cross-linking. And it remains to be seen if the pronounced

scattering at the first sharp diffraction peak reported by S. Hosokawa [54] in anomalous x-ray absorption studies on Ge-Se glasses in the thermally reversing window compositions is actually a manifestation of the filamentary structures.

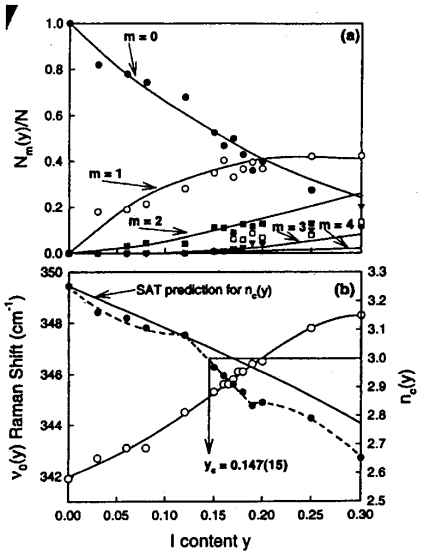

Fig. 11a). Concentration $N_m(y)/N$ of the mixed tetrahedra, m = 0, 1, 2, 3 ,4, plotted as a function of y in the $Ge_{0.25}S_{0.75-y}I_y$ ternary. The smooth curves are the prediction of simple combinatorial calculation (Ref. 7) and are not a fit to the data points. (b) Raman mode frequency variation $n_0(y)$ of m = 0 units and the Raman count of mean-field constraints per atom $n_c(y)$ (Ref. 7), plotted as a function of I content. The smooth line is the stochastic agglomeration theory prediction for $n_c(y)$.

5. Photomelting of the intermediate phase

Semiconducting glasses when illuminated by near band-gap radiation can alter the molecular structure of the intermediate phase. We have carried forward detailed micro- as well as macro-Raman scattering measurements o the same batch of Ge_xSe_{1-x} glasses. In both sets of experiments [41], the back-scattering was excited with the weakly absorbing red light of 647.1 nm radiation from a Kr-ion laser, and the power levels kept in the 500μW range for the micro-Raman and 5 mW range for the macro-Raman measurements. In the micro-Raman measurements the exciting light is brought to a sharp focus of less than 5μ spot size using a microscope with 80x objective in a model T64000 triple monochromater Raman scattering facility from Instruments, S.A., Inc. On the other hand, in the macro-Raman measurements, the exciting light is brought to a loose focus of about 1mm spot size using a macrochamber in the same scattering facility. The spot-size reduction by at least two orders of magnitude translates into an approximately four orders of magnitude reduction in the photon flux (number of photons/cm^2/sec) used to excite the Raman scattering in the macro-configuration (10^{18} photons/cm^2/s) in relation to the micro-configuration (10^{22} photons/cm^2/sec).

Fig.s 12a (Fig. 6 repeated) and 12b show the compositional dependence $\nu_{CS}(x)$ of the CS $Ge(Se_{1/2})_4$ mode frequency observed in Ge_xSe_{1-x} glasses obtained under low and high flux density radiation configurations, respectively, to excite the Raman scattering. The striking difference between Figs. 12a and 12b is the collapse of the intermediate phase which originally extended from $x_c(1)$ = 0.20 to $x_c(2)$ = x = 0.26 down to a single transition point at x_c = 0.23. At both $x_c(2)$ and x_c, $\nu_{CS}(x)$ shows an apparent jump or discontinuity, after which it increases as a power-law that is characteristic of increasing structural stress. Correspondingly, the floppy-phase region is extended from $x_c(1)$ up to x_c.

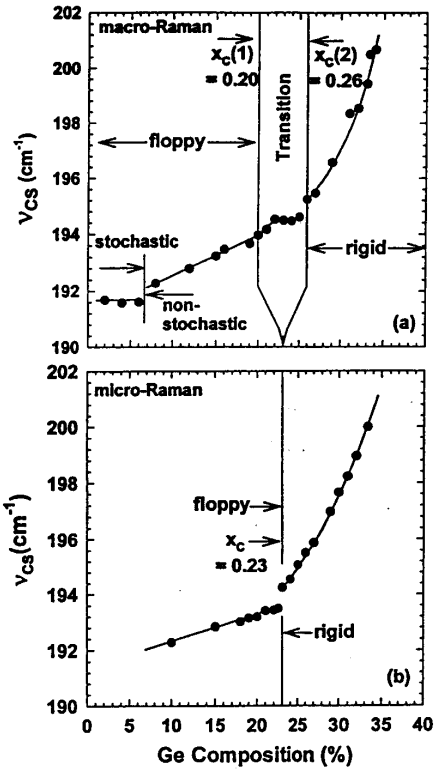

Fig. 12. Corner-sharing mode frequency variation, $n_{CS}(x)$, in Ge_xSe_{1-x} glasses from low intensity (macro-) (a) and high intensity (micro-) Raman (b) measurements. In the latter the intermediate phase collapses to a single point.

The high-flux density illumination clearly has induced changes in chemical bonding, resulting in a *photo-melt*. In either the floppy phase or the rigid phase in the photo-melted state, the overall variation of ν_{CS} is seen to differ little from the behavior in the original glass. We argue that this indicates that chemical bonding of fourfold coordinated Ge and twofold coordinated Se atoms is originally random enough in these phases so that further randomization by the exciting light only produces statistically similar structures. (It is also possible that melting does not occur at all in the floppy and rigid phases at the flux densities of our experiments because ΔH_{nr} is too large but occurs selectively in the intermediate phase where ΔH_{nr} is very small.

The intermediate-phase structure is destroyed presumably by randomization of the bond-distribution. This is suggested by our earlier interpretation of the intermediate phase (following the calculations [23] of Thorpe et al.) as being an *isostatic* structure with no redundant bonding, i.e., no bonding over that required to produce rigidity. This means that an *isostatic* bond configuration is highly *non-random*, since bonds that would be redundant are "repelled". This repulsion can be maintained as we increase the bond density $\bar{r}$ up to the point where the local chemistry can no longer be satisfied without any redundancy. Then a first order transition to a stressed backbone occurs.

In contrast, the randomly bonded structure in the photo-melted state will be floppy up to the concentration x_c where the first rigid (and stressed) backbone develops – in accordance with the original floppy-to-rigid-transition picture proposed by Phillips and Thorpe in the early 1980's. (We note, however, that $x_c = 0.23$ here corresponds to $r_c = 2.46$, a value somewhat larger than the mean-field constraint counting value, $\bar{r}_c = 2.40$ because some of the constraints are intrinsically broken [16]).

Let us engage the notion of *isostacy* to further understand the differences between Fig. 12a and Fig. 12b. Note first that, because of bond repulsion, isostatic structures are more efficiently

packed than randomly bonded structures in achieving a percolating backbone, that is, they require fewer Ge cross-linking atoms; so that $x_c(1)$, the lowest bond density to reach rigidity, will be less than x_c, the lowest value for redundant structures. Under photo-melting, these more efficient structures disappear and rigidity only reappears at the higher value x_c. Between x_c and $x_c(2)$, the corner-sharing $Ge(Se_{1/2})_4$ tetrahedra in the *isostatic* phase will reside mostly in unstressed local environments so that $\nu_{CS}(x)$ will remain constant. At this point we recall that the calculations of Thorpe et al. [23] show that a majority of the atoms are in the backbone as soon as it is formed and that only a small number of added redundant bonds are required for converting the backbone structure to a stressed phase. Thus the change in ν_{CS} at either x_c or $x_c(2)$ is essentially discontinuous and, between these two concentrations, the photo-melted state will have redundant bonds with attendant stressed rigidity.

We conclude this section with two remarks. The present observations suggest that the microscopic origin of the giant photocontraction effects observed by K. L. Chopra et al. [9, 55] in thin-films of $GeSe_2$ may actually represent photomelting of the columnar structure peculiar to the films deposited at high obliqueness angles. The films at high obliqueness angles are intrinsically phase separated on a molecular scale into Se-rich columns and Ge-rich intercolumnar material and the role of illumination is to cause an irreversible photomelting of the stress-free, optimally coordinated columns, as will be shown in a forthcoming publication [56].

The observation of photomelting of As_2S_3 fibers by sub-bandgap (green) radiation reported by K. Tanaka appears to represent photomelting of the intermediate phase in As-S binary glasses. Compositional windows defining the *intermediate phase* in the group V chalcogenides shown that although the stoichiometric glass compositions As_2Se_3 and As_2S_3, are not part of the intermediate phase, these are not sufficiently far removed from that phase, not to show photomelting effects completely.

6. Concluding remarks

The physical behavior of prototypical network glasses, examined systematically as a function of chemical composition, or mean coordination number $\bar{r}$, shows the existence of two compositions ($\bar{r}_c(1)$, $\bar{r}_c(2)$) across which the *elastic*, *thermal*, and *structural* behavior appears to display a threshold behavior. Raman scattering measurements show existence of elastic thresholds at $\bar{r}_c(1)$ and $\bar{r}_c(2)$ with distinct power-laws, which when analyzed in terms of numerical simulations in random- and self-organized network, reveal that glasses at low $\bar{r}$ ($\bar{r} < r_c(1)$), are *floppy*, in the *intermediate* composition interval ($\bar{r}_c(1) < \bar{r} < \bar{r}_c(2)$) are *isostatically rigid*, and at high $\bar{r}$ ($\bar{r} > r_c(2)$) *stressed rigid*. T-modulated DSC measurements of the non-reversing heat flow term, ΔH_{nr} ($\bar{r}$), show a global minimum in the $\bar{r}_c(1) < \bar{r} < \bar{r}_c(2)$ interval with the heat flow term increasing by almost *an order of magnitude* in the *floppy-phase* ($\bar{r} < \bar{r}_c(1)$) and in the *stressed rigid phase* ($\bar{r} < \bar{r}_c(2)$). The activation energy of viscosity $E_\eta^A(\bar{r})$ for corresponding liquids mimics compositional trends in ΔH_{nr} ($\bar{r}$) and shows a *global minimum* in the intermediate phase. Furthermore, T-dependence of viscosity for glass (liquid) compositions in the intermediate phase display an *Arrhenius behavior*, in sharp contrast to the non-Arrhenius behavior encountered in both the floppy- and stressed-rigid phases. Compositional trends in molar volumes, $V_M(\bar{r})$ of glasses also reveal a global minimum [29] in the intermediate phase, suggesting that the underlying network structure are rather efficiently packed.

These experimental findings suggest that glasses in the intermediate phase consist of networks that are optimally constrained and self-organized, those in the floppy phase are underconstrained and entropically stressed while those in the stressed rigid-phase are mechanically overconstrained and enthalpically stressed.

The width ($r_c(2) - r_c(1)$) and centroid ($r_c(1) + r_c(2)$)/2 of the intermediate phase in $\bar{r}$ space, observed in several chalcogenide and chalcohalide glasses shows that these $\bar{r}$ values are manifestations of structure at a *short-range* and at a *medium-range* distances. For the case of the chalcohalide glass system, $Ge_{0.25}S_{0.75-y}I_y$, where the evolution of glass structure as a function of iodine content is found to be truly *stochastic*, the *width* of the intermediate phase *vanishes* and a *solitary* rigid to floppy transition is documented at a composition ($y = y_c = 1/6$). The result is in excellent

agreement with mean-field constraint counting algorithms extended to include networks with dangling ends. In the case of this chalcohalide glass system, the stochastic evolution of glass structure precludes self-organization and opening of an intermediate phase. In return, the existence of intermediate phases with significant width $r_c(2) - r_c(1)$ in binary and ternary chalcogenide glasses shows that the optimally constrained backbone displays substantial self-organization. And it is possible that the latter may consist of filamentary structural elements that are qualitatively decoupled from each other.

Acknowledgements

One of us (PB) would like to thank M. Popescu for the invitation to participate in the 1st Amorphous and Nanocrystalline Chalcogenide Workshop held in Bucharest. Y. Wang, D. Selvanathan, W. J. Bresser and J. Wells assisted in the experiments described in this review. We have benefited with on-going discussions with J. C. Phillips, M. F. Thorpe, M. Micoulaut and K. A. Jackson in the course of this work. This work is supported by National Science Foundation grant DMR-01-01808.

References

[1] A. C. Angell in Insulating and Semiconducting Glasses, Ed. P. Boolchand, World Scientific Press, Inc., Singapore, 2000.
[2] E. C. Weeks, J. R. Croker, A. C. Levitt, A. Schofield, D. A. Weitz, Science **287**, 627 (2000). Also see A.C. Wright in Insulating and Semiconducting Glasses, Ed. P. Boolchand, World Scientific Press, Inc., Singapore, p. 147, 2000.
[3] P. Boolchand in Insulating and Semiconducting Glasses, Ed. P. Boolchand, World Scientific Press, Inc., Singapore, p. 191, 2000.
[4] P. Boolchand, D. Selvanathan, Y. Wang, D. G. Georgiev, W. J. Bresser in Properties and Applications of Amorphous Materials, Ed. M. F. Thorpe, L. Tichy, Kluwer Academic Publishers, Dordrecht, p. 97, 2001.
[5] Y. Wang, P. Boolchand, M. Micoulaut, Europhysics Letters **52**, 633 (2000).
[6] D. Selvanathan, W. J. Bresser, P. Boolchand, Phys. Rev. **B61**, 15061 (2000). Also see Solid State Commun. **111**, 619 (1999).
[7] Y. Wang, J. Wells, D. G. Georgiev, P. Boolchand, K. A. Jackson, M. Micoulaut, Phys. Rev. Lett. (in press).
[8] H. Hisakuni, K. Tanaka, Science **270**, 974 (1995).
[9] K. L. Chopra, K. S. Harshavardhan, S. Rajgopalan, L. K. Malhotra, Solid State Commun. **40**, 387 (1981).
[10] C. A. Angell, K. L. Ngai, G. B. McKenna, P. F. McMillan, S. W. Marti, Appl. Phys. Rev. **88**, 3113 (2000).
[11] J. C. Phillips, J. Non Cryst. Solids **34**, 153 (1979).
[12] M. F. Thorpe, J. Non Cryst. Solids **57**, 355 (1983).
[13] M. F. Thorpe, M. V. Chubynsky in Properties and Applications of Amorphous Materials, Ed. M. F. Thorpe, L. Tichy, Kluwer Academic Press, Dordrecht, p. 61, 2001.
[14] H. He, M. F. Thorpe, Phys. Rev. Lett. **54**, 2107 (1985).
[15] D. S. Franzblau, J. Tersoff, Phys. Rev. Lett. **68**, 2172 (1992).
[16] X. W. Feng, W. J. Bresser, P. Boolchand, Phys. Rev. Lett. **78**, 4422 (1997).
[17] M. Zhang, P. Boolchand, Science **266**, 1355 (1994).
[18] R. L. Mozzi, B. E. Warren, J. Appl. Crystallogr., **2**, 164 (1969).
[19] J. C. Phillips, Solid State Commun., **47**, 203 (1983).
[20] M. Stevens, J. Grothaus, P. Boolchand, Solid State Commun., **47**, 199 (1983).
[21] P. Boolchand, M. F. Thorpe, Phys. Rev., **B50**, 10366 (1994).
[22] P. Boolchand, M. Zhang, B. Goodman, Phys. Rev., **B53**, 11488 (1996).
[23] M. F. Thorpe, D. J. Jacobs, M. V. Chubynsky, J. C. Phillips, J. Non Cryst. Solids, **266-269**, 872 (2000).

[24] Y. Wang, M. Nakaravra, O. Matsuda, K. Murase, J. Non Cryst. Solids, **266-269**, 872 (2000).
[25] Y. Vaills, Y. Luspin, G. Hauret, Mat. Sci. Eng., **B40**, 199 (1996).
[26] For Mössbauer Lamb-Mössbuaer factors see: P. Boolchand, W. Bresser, M. Zhang, Y. Wu, J. Wells, R.N. Enzweiler, J. Non Cryst. Solids, **182**, 143 (1995). For neutron scattering work see: W. A. Kamitakahara, R. L. Cappelletti, P. Boolchand et al. Phys. Rev., **B44**, 94 (1991).
[27] R. Bohmer, C. A. Angell, Phys. Rev., **B45**, 1091 (1992).
[28] U. Senapati, A. K. Varsheneya, J. Non Cryst. Solids, **185**, 289 (1995).
[29] A. Feltz, H. Aust, A. Blayer, J. Non Cryst. Solids, **55**, 179 (1983). For work on other chalcogenides also see: S. Mahadevan, A. Giridhar, J. Non Cryst. Solids, **152**, 42 (1993).
[30] S. Asokan, M. Y. N. Prasad, G. Parathasarthy et al. Phys. Rev. Lett., **62**, 808 (1989).
[31] R. A. Narayan, S. Asokan, A. Kumar, Phys. Rev., B**63**, 092203.
[32] T. Wagner, S. O. Kasap, K. Maeda, J. Mat. Research, **12**, 1892 (1997); also see Reprint #TA-210, T.A. Instruments, Inc., New Castle, Delaware.
[33] D. G. Georgiev, M. Mitkova, P. Boolchand, H. Brunklaus, H. Eckert, M. Micoulaut, Phys. Rev. B (in press).
[34] D. G. Georgiev, P. Boolchand, M. Micoulaut, Phys. Rev., B**62**, R9228 (2000).
[35] R. Kerner, M. Micoulaut, J. Non Cryst. Solids, **176**, 271 (1994).
[36] D. Lathrop, H. Eckert, J. Phys. Chem., **93**, 7895 (1989).
[37] F. L. Galeener, J. Non Cryst. Solids **123**, 182 (1990).
[38] G. Lucovsky, Solid State Commun., **29** 571 (1979).
[39] J. E. Griffiths, G. P. Espinosa, J. P. Remeika et al. Phys. Rev., B**25**, 1272 (1982).
[40] K. Murase, Insulating and Semiconducting Glasses, Ed. P. Boolchand, World Scientific Press, Inc., Singapore, 2000, p. 415.
[41] P. Boolchand, X. W. Feng, W. J. Bresser, J. Non Cryst. Solids (in press).
[42] J. T. Chayes, L. Chayes, D. S. Fisher et al. Phys. Rev. Lett. **57**, 2999 (1986).
[43] M. Micoulaut, Eur. Phys. J., **B1**, 277 (1998).
[44] W. J. Bresser, P. Boolchand, P. Suranyi, Phys. Rev. Lett. **56**, 2493 (1986).
[45] M. F. Thorpe, D. J. Jacobs, N. V. Chubynsky, A. J. Rader in Rigidity Theory and Applications, Ed. M. F. Thorpe and P. M. Duxbury, Kluwer Academic/Plenum Publishers, p. 39, 1999.
[46] C. F. Mourkazel, P. M. Duxbury in Rigidity Theory and Applications, Ed. M. F. Thorpe and P. M. Duxbury, Kluwer Academic/Plenum Publishers, p. 69, 1999.
[47] P. Boolchand in Insulating and Semiconducting Glasses, Ed. P. Boolchand, World Scientific Press, Inc., Singapore, p. 369, 2000.
[48] For a recent review of the subject see, P.G. Debenedetti and F.H. Stillinger in Nature, **410**, 259 (2001).
[49] C. A. Angell, Science, **267**, 1924 (1995).
[50] S. V. Nemilov, G. T. Petrovckii, Zh. Prikl. Khim., **36**, 977 (1963).
[51] M. Mitkova, P. Boolchand, J. Non Cryst. Solids, **240**, 1 (1998).
[52] S. A. Dembovsky, V. V. Kirilenko, Y. A. Buslaev, Neorg. Mater., **7**, 328 (1971).
[53] K. A. Jackson, A. Briley, S. Grossman, D. V. Porezag, M.R. Penderson, Phys. Rev., B**60**, R14985 (1999).
[54] S. Hosokawa, J. Optoelectronics and Advanced Mat., **3**, 199 (2001) and references therein.
[55] See S. Rajgopalan, B. Singh, P. K. Bhat, D. K. Pandya, K. L. Chopra, J. Appl. Phys., **50**, 489 (1979).
[56] P. Boolchand, W. J. Bresser, T. Rajgopalan, K. L. Chopra (unpublished).